Evaluating Smooth Muscle Cells from CaCl$_2$-Induced Rat Aortal Expansions as a Surrogate Culture Model for Study of Elastogenic Induction of Human Aneurysmal Cells

Carmen Gacchina, Ph.D.,[1,2] Thomas Brothers, M.D.,[3] and Anand Ramamurthi, Ph.D.[1,2,4]

Regression of abdominal aortic aneurysms (AAAs) via regeneration of new elastic matrix is constrained by poor elastin synthesis by adult vascular cells and absence of methods to stimulate the same. We recently showed hyaluronan oligomers (HA-o) and TGF-β1 (termed elastogenic factors) to enhance elastin synthesis and matrix formation by healthy rat aortic smooth muscle cells (RASMCs). We also determined that these factors could likewise elastogenically induce aneurysmal RASMCs isolated from periadventitial CaCl$_2$-injury induced rat AAAs (aRASMCs). However, the factor doses should be increased for these diseased cell types, as even when induced, elastic matrix amounts are roughly one order of magnitude lower than those produced by healthy RASMCs. We presently investigate the dose-specific elastogenic effects of HA-o (0–20 μg/mL) and TGF-β1 (0–10 ng/mL) factors on aRASMCs and compare their phenotype and elastogenic responses to those of human AAA-derived SMCs (aHASMCs); we seek to determine whether aRASMCs are appropriate surrogate cell types to study in the context of inducing elastic matrix regeneration within human AAAs. The periadventitial CaCl$_2$-injury model of AAAs exhibits many of the pathological characteristics of human AAAs, including similarities in terms of decreased SMC contractile activity, enhanced proliferation, and reduced elastogenic capacity of aneurysmal SMCs (relative to healthy SMCs) when isolated and expanded in culture. Both aRASMCs and aHASMCs can be elastogenically stimulated by HA-o and TGF-β1 and show broadly similar trends in their dose-specific responses to these factors. However, compared with aHASMCs, aRASMCs appear to be far less elastogenically inducible. This may be due to differences in maturity of the AAAs studied, with the CaCl$_2$-injury induced aortal expansion barely qualifying as an aneurysm and the human AAA representing a more well-developed condition. Further study of SMCs from stage-matched CaCl$_2$-injury induced rat aortal expansions and human AAAs will be necessary to more rigorously evaluate their basal and induced elastogenic responses.

Introduction

ELASTIC FIBERS in the extracellular matrix (ECM) of vascular tissues provides them elasticity and resilience. In addition, intact elastic fibers maintain vascular smooth muscle cells (SMCs) in a healthy, quiescent, contractile phenotype. In certain pathological conditions, such as aneurysms of the abdominal aorta (AAAs), accelerated elastic fiber breakdown leads to segmental dilation of the aortal wall, loss of elasticity, and potentially fatal vessel rupture.[1] AAAs typically initiate on recruitment of inflammatory cells (e.g., macrophages) in response to lipid deposition and calcification within the abdominal aortic wall.[2] The inflammatory cells release matrix-metalloprotease (MMP) enzymes that breakdown elastin to generate soluble elastin peptides.[3]

These peptides, different from intact elastic fibers, activate medial SMCs and prompt their secretion of cytokines, chemokines, interleukins, and proteinases that propagate the cycle of matrix degradation.[4,5] This ultimately leads to loss of elasticity and strength of the aortic wall and its progressive dilation to form a rupture-prone sac of weakened tissue.[1] Clearly, the breakdown of elastic matrix structures contributes to AAA formation and growth, among other vital factors such as chronically elevated local MMP production and activity.

Due to complications that adversely impact immediate and long-term survival after open surgical AAA repair and endovascular aneurysm repair,[6] there has been an interest in developing nonsurgical AAA therapies. Treatment modalities under study include pharmacological inhibition of MMP

---

[1]Clinical Center, National Institutes of Health, Bethesda, Maryland.
[2]Department of Bioengineering, Clemson University, Clemson, South Carolina.
[3]Department of Surgery, Medical University of South Carolina, Charleston, South Carolina.
[4]Department of Biomedical Engineering, Cleveland Clinic, Cleveland, Ohio.

production and activity within AAAs using tissue inhibitors of matrix metalloproteases (TIMPs)[7] and modified tetracyclines,[8] and chemical crosslinking of existing aortal elastic matrix structures .[9,10] Unfortunately, these strategies do not concurrently restore healthy cell phenotypes, reinstate healthy elastic matrix, and provide conditions for stabilizing the local vascular environment. *In situ*, cell-mediated regeneration of elastic matrix structures within intact AAAs could achieve these objectives for possible regression of AAAs. However, such regeneration is challenging, as adult vascular SMCs poorly synthesize elastin or remodel mature elastic fibers.

In an earlier study, we identified a unique cocktail of elastogenic factors, namely hyaluronan oligomers (HA-o; 4–6 mers; 756 Da)[11,12] and growth factors (TGF-β1).[13,14] We showed that these elastogenic factors synergistically deter rat aortic SMC (RASMC) proliferation, enhance tropoelastin (elastin precursor) synthesis and recruitment, fiber maturation, and stability. We recently showed that the same factors, provided at doses optimized for healthy cells (2 μg/mL HA-o and 1 ng/mL TGF-β), likewise elastogenically stimulate SMCs isolated from CaCl2-injury induced rat aortal expansions (aRASMCs).[15] This study provided preliminary evidence that aRASMCs continue to exhibit a diseased/ activated phenotype in culture and that they can be elastogenically stimulated. However, the study also emphasized the need to increase factor doses for elastogenic stimulation of the diseased cells, as induced elastic matrix productionis an order of magnitude less than that produced by healthy RASMCs. This shortcoming is addressed in the present study.

Although the therapeutic efficacy of biomolecular factors should be necessarily demonstrated in animal models of disease before testing in human subjects, we should also ascertain whether outcomes with the surrogate model/cell type will parallel outcomes in humans. We have, thus, compared dose-specific elastogenic effects of HA-o and TGF-β in cultures of SMCs isolated from CaCl2-induced rat AAAs and SMCs isolated from atherosclerotic human AAA tissue (aHASMCs).

Materials and Methods

Aortal injury by periadventitial application of CaCl2

All animal studies were approved by the IACUC at the Medical University of South Carolina, where this work was performed before relocation of the primary investigators. Adult Sprague-Dawley rats (250–300 g in weight) were procured and acclimatized for 1 week before surgery. The rats were placed under general anesthesia (2%–3% v/v isoflurane), and the infrarenal abdominal aortae were surgically exposed. The aortae were treated using a previously described protocol.[16,17] Briefly, sterile cotton gauze presoaked with 0.5 mol/L CaCl2 was placed periadventitially on the aorta for 15 min. Sufficient care was taken not to injure surrounding organs by exposure to caustic CaCl2. The abdominal cavity was then washed with sterile saline to remove residual CaCl2.Then, the cavity was closed, subcutaneously sutured, and stapled; and the rats were allowed to recover. At 28 days postinjury with CaCl2, the animals were euthanized by CO2 asphyxiation. The expanded infrarenal abdominal aortae were then excised and processed for isolation

of SMCs. The abdominal aortae were photographed before CaCl2 exposure, and at 28 days after to compare the changes in aortic diameter. Histological analysis and MMP zymography were conducted on the expanded aortal tissue to confirm AAA formation.

To verify medial disruption and thinning, and calcific deposition within the aortic wall of CaCl2-treated animals, standard hematoxylin and eosin staining (for nuclear and intracellular and extracellular protein visualization), modified Verhoff Van Gieson staining (VVG; for elastin visualization; ScyTek Laboratories, Logan, UT), Von Kossa staining (for calcific depostion; ScyTek Laboratories), and scanning electron microscopy (SEM; for aortic cross-section ultrastructural visualization) were conducted on untreated aortae (control) and CaCl2-treated aortae (n = 3 animals/group). Aortae from rats harvested at 28 days postop (or at a timematched stage for unoperated control animals) were rinsed in sterile saline, embedded in optimum cutting temperature medium, and stored at −20°C. Cryoections (5μm) were processed for histology or SEM. Standard histological protocols were followed. For SEM, samples were fixed in 2% v/ v gluteraldehyde in phosphate buffer, rinsed in phosphate buffer, deionized (DI) water, and then dehydrated in graded ethanol and finally hexamethyldisilazane (Sigma Aldrich, St. Louis, MO) (3 min). Histological and SEM imaging was performed on an Olympus BX41 (Olympus, Center Valley, PA) and a Hitachi SEM TM1000 (Hitachi Technologies, Pleasanton, CA), respectively.

Isolation and culture of aRASMC and aHASMC

Expanded aortae isolated from rats (n = 3) that were subject to periadventitial injury with CaCl2 were opened lengthwise, and the intima scraped off gently with a scalpel blade. The medial layer was dissected from the underlying adventitia, chopped into ∼0.5 mm-long sections, and washed twice with warm phosphate-buffered saline (PBS). The tissue slices were then pooled, enzymatically digested in DMEM-F12 (Invitrogen, Grand Island, NY) containing 125 U/mg collagenase type II (1 mg/mL; Worthington, Biochemicals Lakewood, NJ) and 3 U/mg elastase (Worthington Biochemicals) for 30 min at 37°C. The digestates were then centrifuged (1400 RPM; 5 min), and the pelleted tissue pieces were cultured in T-75 flasks with DMEM-F12 containing 10% v/v fetal bovine serum (FBS; PAA Laboratories, Etobicoke, Ontario, CA) for more than 15 days. Primary aneurysmal aRASMCs derived by outgrowth from these tissue explants were cultured for up to 2 weeks, and the cells were passaged when confluence was attained. For culture studies, passage 3 SMCs were seeded onto six-well tissue culture plates (growth area of 9.6 cm^2) at a density of 2×10^4 cells/well and cultured in DMEM-F12 medium containing 10% v/v FBS and 1% v/v penstrep. The total volume of medium added per well was 5 mL.

Waste human AAA tissue, generated during open AAA repair (Fig. 3B), was procured with IRB approval at the Medical University of South Carolina (HR# 18387, 07/2008). The tissue source was a 6 cm diameter AAA from a 62-yearold male patient with hypertension, coronary disease, and hyperlipidemia. The tissue, which exhibited significant thrombus formation, was collected from the anterior wall of the aneurysm near the origin of the inferior mesenteric

artery. After explanting the aneurysmal tissue, the AAA was successfully repaired in a standard fashion. To isolate primary aneurysmal human aortic SMCs (aHASMCs), the 4×1-cm-sized aortic tissue explant was opened lengthwise, the intima scraped with a scalpel blade, the medial layer dissected from the adventitia, and then chopped it into ~ 0.5 mm-long sections. Subsequently, the pieces were rinsed with sterile PBS, pooled, and enzymatically digested in DMEM-F12 medium (Invitrogen) containing 357 U/mg collagenase type II and 4.5 U/mg elastase (both from Worthington Biochemicals) for more than 45 min at 37°C. The digestate was centrifuged (1400 RPM; 5 min), and the tissue fragments were then re-constituted and cultured for up to 6 weeks in six-well plates with minimal volumes of DMEM-F12 medium containing 10% v/v FBS. Primary aHASMCs, derived by outgrowth from these tissue explants, were cultured until confluence was attained and then passaged. Passage 3 aHASMCs were then seeded onto six-well tissue culture plates at a density of 2×10^4 cells/well and cultured in DMEM-F12 supplemented with 5% v/v FBS, 1% v/v penstrep, 5 μg/mL human insulin (Sigma, St. Louis, MO), 2 ng/mL of human recombinant fibroblast growth factor (Peprotech, Rocky Hill, NJ), and 0.5 ng/mL of human recombinant epidermal growth factor (Assay Design, Ann Arbor, MI). Passage-matched healthy HASMCs isolated from fibrous plaque-free aorta of a 48-year-old Caucasian male (HASMCs; Cell Applications, San Diego, CA) were also cultured under identical conditions.

Experimental design and time points

Passage 3 aRASMCs, aHASMCs, and healthy HASMCs were cultured in medium supplemented with elastogenic factors (0, 0.2, 2, and 20 μg/mL HA-o and 0, 1, 5, and 10 ng/mL TGF-β) within six-well plates (2×10^4 cells/9.6 cm^2) for 21 days, over which time the cells deposited a robust matrix. Spent medium aliquots were removed from each well, at the time of each twice-weekly medium change. The aliquots from each well were pooled with previously removed aliquots from the same wells, frozen at -20°C, and then biochemically assayed together with their corresponding cell layers when harvested at 21 days of culture.

DNA assay for cell proliferation

The DNA contents of each group of cell cultures were compared to determine the impact of the factors and factor doses on SMC proliferation. For analysis, the cell layers were harvested at 21 days of culture, resuspended in NaCl-Pi buffer, and sonicated on ice. The DNA contents of the respective samples were quantified using a fluorometric assay described by Labarca and Paigen.[18] Cell counts were then calculated assuming 6 pg of DNA/cell.[18]

Immunofluorescence detection of SMC phenotypic markers

Immunofluorescence was used to visually compare contractile and synthetic phenotypic marker expression between aneurysmal and healthy HASMCs, and aneurysmal and healthy RASMCs. SMCs were cultured in sterile, two-well Permanox® chamber slides (4.2 cm^2/well; Nalge Nunc International, Rochester, NY) under identical experimental conditions as described for cultures intended for biochemical analysis, though the number of cells seeded and treatment doses were adjusted, to account for the reduced substrate surface area and cell number, respectively. The cell layers were fixed with acetone for 10 min at -20°C and blocked with 5% v/v goat serum (30 min). α-Smooth muscle actin, SM22α, calponin, caldesmon (contractile phenotype markers), and thrombospondin and osteopontin (synthetic phenotype markers) were then detected with polyclonal antibodies against rat antigens (1:100 v/v; Abcam, Cambridge, MA), which also cross-react with human antigens, and visualized with FITC-conjugated IgG secondary antibodies (1:1000 v/v; Chemicon, Temecula, CA). The cell layers were cover-slipped with Vectashield mounting medium containing the nuclear dye 4′,6-diamidino-2-phenylindole (DAPI; Vector Laboratories, Burlingame, CA), which labeled the cell nuclei.

Flow cytometry

In preparation for flow cytometry, SMCs (passage 3) were trypsinized, centrifuged (1500 RPM; 10 min), re-constituted at 1×10^6 cells per sample, fixed with 4% w/v paraformaldehyde in PBS (37°C; 10 min), washed, and then permeabilized with 0.1% v/v Triton X-100 in PBS for 1 min. Immunofluorescence detection of SMC phenotypic markers was conducted with the antibodies listed in Immunoflourescence detection of SMC phenotypic markers section. The samples were blocked (30 min; 4°C), then incubated with primary antibodies (30 min; 4°C), followed by an FITC-conjugated secondary antibody (20 min; 4°C; in the dark). After labeling, cells were re-suspended in 0.5 mL of PBS and kept at 4°C, in the dark, until analysis. Cytometric analysis was performed using a Becton Dickinson FACSCalibur Analytical Flow Cytometer, and data were processed using Cell Quest Pro 5.2 (BD Biosciences, Franklin Lakes, NJ).

Fastin assay for elastin

The Fastin assay (Accurate Scientific and Chemical Corporation, Westbury, NY) was used to quantify the total amount of elastin deposited within cell layers (matrix elastin), and the elastin was released into the culture medium as a soluble precursor (tropoelastin). For each treatment group, tropoelastin in the spent medium was collected, pooled over the culture period, and frozen at -20°C. To isolate matrix elastin after 21 days, the cell layers were trypsinized, then scraped off, re-suspended in NaCl/Pi buffer, and centrifuged (2500 RPM, 10 min). The cell pellet was digested with 0.1 N NaOH (98°C, 1 h) and centrifuged to yield a less crosslinked, alkali-soluble supernatant fraction (soluble elastin), and a mature, highly crosslinked, insoluble pellet (insoluble elastin). Since the Fastin assay quantifies only soluble α-elastin, the insoluble elastin was converted to a soluble form before quantification. To do this, the insoluble elastin pellet was dried, solubilized with 0.25 M oxalic acid (95°C, 1 h), and the pooled digests were then centrifuge-filtered (3000 RPM, 10 min) in microcentrifuge tubes fitted with low molecular weight (10 kDa) cut-off membranes (Millipore, Bedford, MA). All three elastin fractions (tropoelastin, and soluble and insoluble matrix elastin) were quantified using the Fastin assay. Our lab has been able to consistently reproduce standard curves generated with serial dilutions of elastin

standards and has also established the linearity of the assay with a dilution series of elastin samples of unknown concentration. This assures of the reproducibility of the assay for elastin quantification.

Von Kossa staining

Von Kossa staining of calcific deposits was used to verify that the TGF-β doses provided did not stimulate matrix calcification by aneurysmal SMCs. SMCs were cultured in sterile, two-well Permanox® chamber slides (Nalge Nunc International) under identical experimental conditions as described for cultures meant for biochemical analysis. Seeding cell numbers and treatment doses were, however, adjusted to account for the reduced substrate surface area and cell number, respectively. After 21 days of culture, SMCs were incubated with 1% w/v silver nitrate solution and placed under UV light ($\lambda = 254$ nm; 20 min). After several changes of distilled water, the unreacted silver was removed by rinsing cells first with 5% w/v sodium thiosulfate for 5 min, then with PBS. The slides were counterstained with hematoxylin. The appearance of black stained masses in the cell layers confirmed the presence of calcium phosphate deposits.

Gel zymography

MMP activity in spent cell culture medium was quantified using gelatin zymography methods as previously described.[15] Briefly, aliquots of culture medium were first assayed for protein content using the BCA assay. All lanes of the gel were then loaded in with equal amounts of protein. A prestained molecular weight standard (BioRad, Hercules, CA) and MMP-2 and −9 standards (Anaspec, San Jose, CA) were also loaded alongside. Such gels were run in triplicate. After development, staining, and destaining, bands from the inactive and active MMP-2 and −9 isoforms appeared on a dark background of stained gelatin, were measured using ImageJ software (NIH, Bethesda, MD), and quantified as relative density units.

MMP array

To assess the MMPs and TIMPs released by aHASMCs as compared with aHASMCs treated with an optimal dose of elastogenic factors, an MMP array was used. Proteins from factor-supplemented and nonfactor supplemented aHASMC cultures were extracted in an RIPA buffer (Thermo Scientific, Waltham, MA), centrifuged (2500 RPM, 5 min), and the supernatant was analyzed using an ELISA-based MMP antibody array (RayBiotech, Norcross, GA). The array identified MMPs-1, −2, −3, −9, −10, −13 and TIMPs-1, −2, −4. The manufacturer's protocol was followed, and the array was imaged on the UVP EC3 BioImaging System (Upland, CA). Since rat MMP arrays are not commercially available, such analysis was not conducted on RASMC cultures.

SEM of elastic matrix

SEM was used to visualize elastic matrix architecture. At 21 days of culture, spent medium was removed from atop cell layers. The cell layers were rinsed with PBS and fixed with 4% w/v paraformaldehyde in 0.1 M phosphate buffer (4°C, 15 min). After fixation, the cell layers were rinsed sev-

eral times with 0.1M phosphate buffer, then submersed in 25% w/v KOH (60°C, 5 min) to remove cellular and ECM debris and yield relatively pure, matrix elastin structures. After a phosphate buffer rinse, the isolated elastic structures were treated with 1% w/v tannic acid (1 h) and stained with osmium tetroxide (1 h), dehydrated successively in graded ethanol (70%–100% v/v; 1 min each), and finally equilibrated with hexamethyldisilazane (Sigma Aldrich) (3 min). The air-dried samples were finally mounted on aluminum stubs and imaged using a Hitachi SEM TM1000 (Hitachi Technologies).

Transmission electron microscopy of elastic matrix

Transmission electron microscopy (TEM) was used to characterize the ultrastructure of the elastic matrix. At 21 days postseeding, all control and test groups were fixed with 2% w/v cacodylate glutaraldehyde (12 h), postfixed in 1% w/v osmium tetroxide (1 h), dehydrated in a graded ethanol series (50%–100% v/v), embedded in Epon 812 resin, sectioned, placed on copper grids, stained with uranyl acetate and lead citrate, and visualized on a Hitachi TEM H7600T (High Technologies, Pleasanton, CA).

Statistical analysis

The experimental data ($n = 3$/case) were analyzed using Student's t-test. Statistical significance was deemed for $p < 0.05$. Asterisks in figures denote statistical significance ($p < 0.05$) for each group compared with nontreated cell cultures of respective types (controls).

Results

Aneurysm progression and SMC phenotype

A ∼45% local increase in rat aortic diameter, typical of an early aneurysm, was attained over a 28 day period after periadventitial CaCl$_2$ exposure. This agrees well with our earlier observations.[15] Detailed histological analysis demonstrated significant medial thinning, elastic matrix disruption, matrix calcification, and involvement of inflammatory cells in the etiology of the expansion (Fig. 1). aRASMCs isolated from CaCl$_2$ injured aortae appeared to comprise a mixed cellular population with a significant number of cells exhibiting decreased volume/spreading. Expression of α-actin, SM-22, caldesmon, and calponin was reduced compared with healthy RASMCs, as illustrated in Figure 2A and 2B, thus suggesting a loss of contractile phenotype. The aRASMCs also exhibited increased expression of osteopontin (Fig. 2B), a marker indicative of a switch to a synthetic phenotype, which SMCs typically express in response to injury.

aHASMCs isolated from atherosclerotic human AAA tissue (Fig. 3B) initially appeared less spread and more spindle-shaped relative to healthy HASMCs (Fig. 3A), although no differences were noted at confluence. Immunofluorescence labeling visually suggested that thrombospondin and osteopontin expression are very poor or nonexistent in HASMC cultures (Fig. 3C), but may be enhanced in aHASMC cultures. FACS analysis of healthy and aneurysmal HASMCs confirmed the latter cell type to exhibit decreased expression of the contractile SMC markers SM22, caldesmon, and calponin expression relative to healthy HASMCs (Fig. 3D). The aHASMCs also showed increased expression of osteopontin, suggesting assumption of a synthetic phenotype.
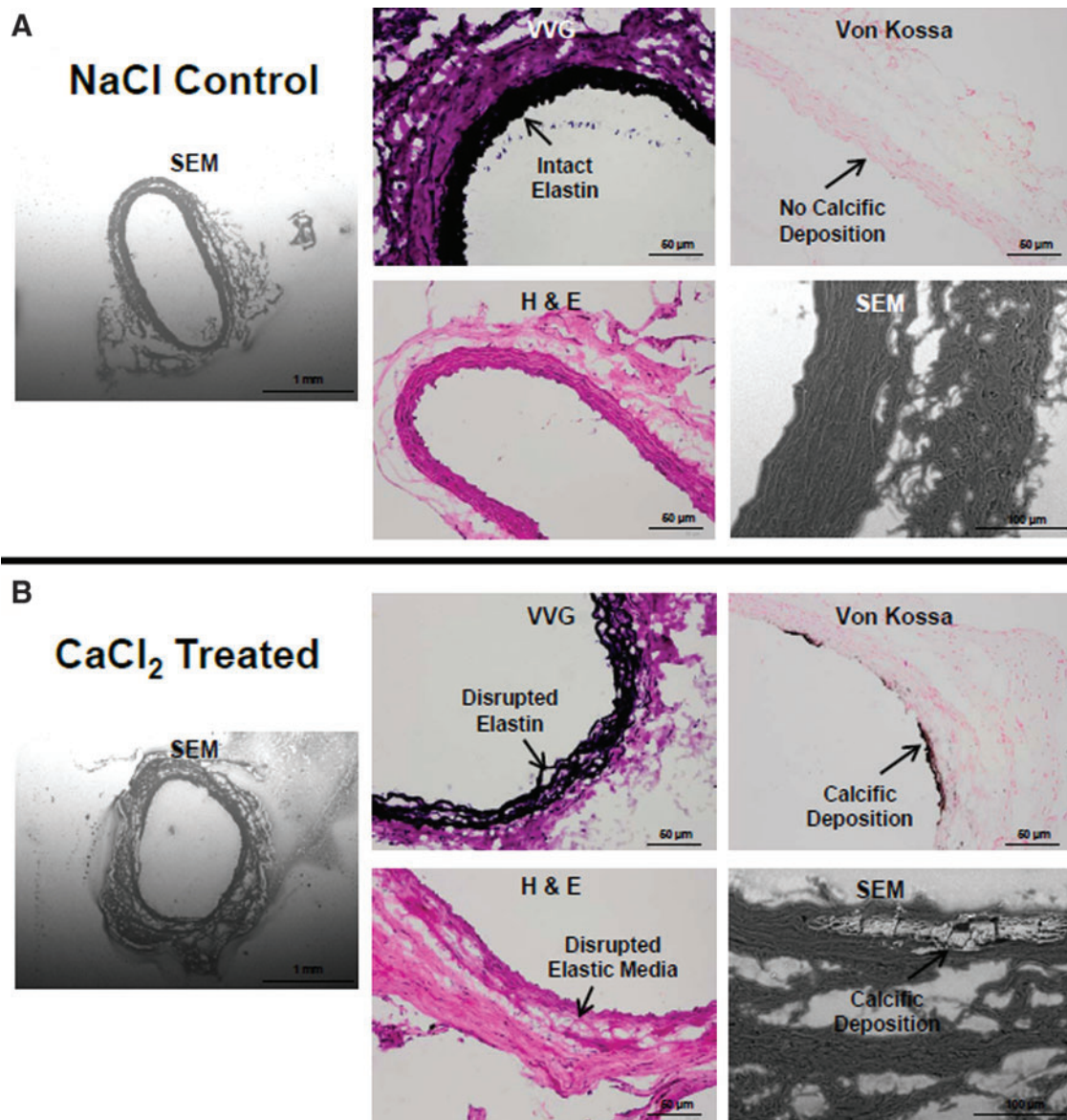
FIG. 1. Representative SEM (50× and 500× magnification) and histological micrographs (VVG, H&E, and Von Kossa; 20× magnification) of CaCl₂-treated aortae **(B)** as compared with control NaCl-treated aortae **(A)**. H&E, hematoxylin and eosin; SEM, scanning electron microscopy; VVG, Verhoff Van Gieson. Color images available online at www.liebertonline.com/tea

aRASMC and aHASMC proliferation

Addition of TGF-β and HA-o had no significant effects on aRASMC proliferation except at a dose of 2 µg/mL HA-o and 10 ng/mL TGF-β, which increased proliferation ($p = 0.002$; Fig. 2C). At higher doses of HA-o (20 µg/mL), cell proliferation ratios were increasingly attenuated with increases in TGF-β dose; there was a significant decrease in cell count, relative to the control, at the highest provided TGF-β dose (10 ng/mL TGF-β; $p = 0.01$) and a significant difference between cell counts within cultures that received the lowest and highest TGF-β doses (1 and 10 ng/mL TGF-β; $p = 0.023$). TGF-β and HA-o also had no significant effect on aHASMC proliferation, at any tested dose (Fig. 3E).

Matrix synthesis

As shown in Figure 4A, most dose combinations of HA-o and TGF-β had no effect on tropoelastin production by aRASMCs. A significant increase in tropoelastin production by aRASMCs was seen only at the highest dose of 20 µg/mL of HA-o and 10 ng/mL of TGF-β, ($p = 0.043$). At this dose, matrix elastin synthesis was also increased, but was not deemed significant from a statistical standpoint. As seen in Figure 4A and 4B, when HA-o and TGF-β were provided to aRASMCs at a moderate dose of 2 µg/mL HA-o and 10 ng/mL TGF-β, no increase in tropoelastin production over controls was measured, though a significant increase in matrix elastin (including both highly cross-linked, alkali-insoluble structural elastin, and an alkali-soluble fraction) was
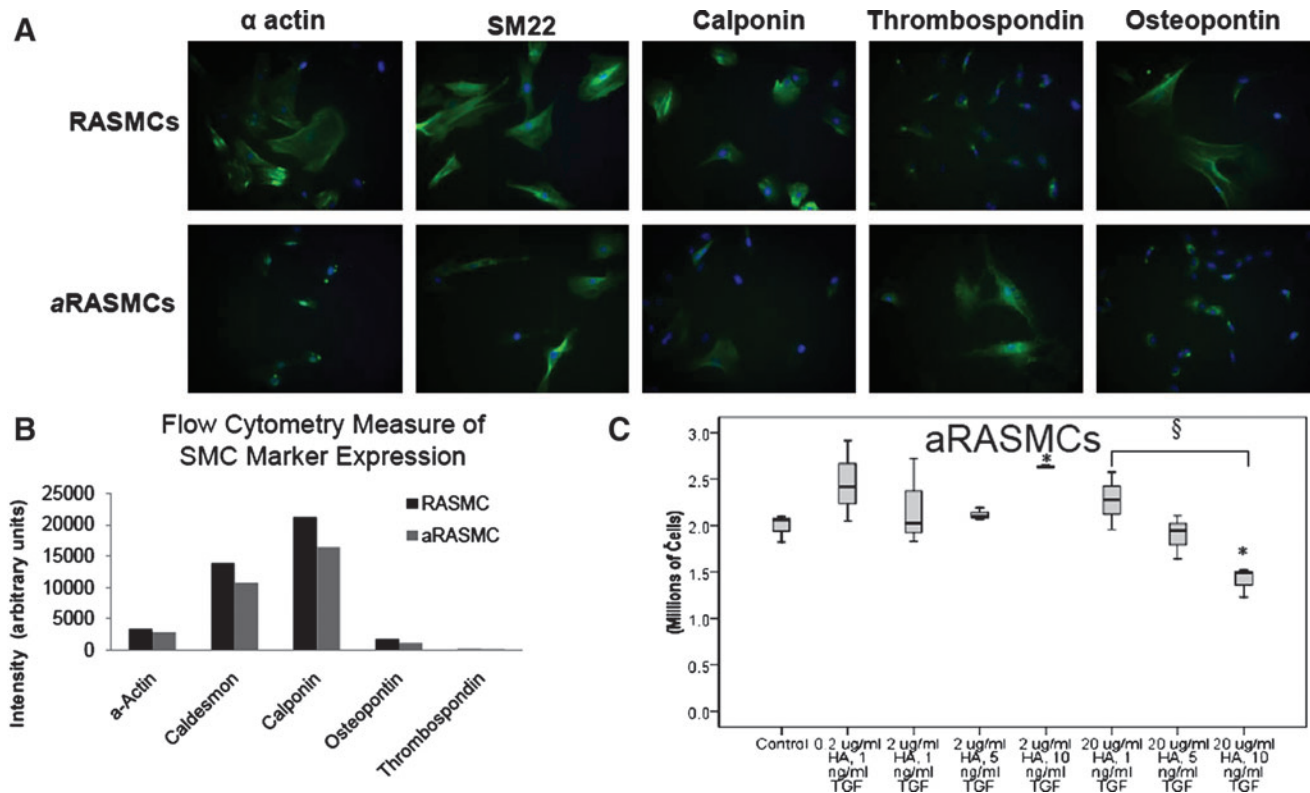
FIG. 2. **(A)** Immunofluorescence images comparing expression of phenotypic markers by RASMCs and aRASMCs. **(B)** Flow cytometry data of RASMC and aRASMC phenotypic marker expression (total intensity of marker expression per 100 cells). **(C)** aRASMC count after 21 days of culture with or without HA-o and TGF-β factor supplementation ($n = 3$/case). *$p < 0.05$ as compared with control; $^{\S}p < 0.05$ as compared with other specified conditions. HA-o, hyaluronan oligomers; RASMCs, rat aortic smooth muscle cells. Color images available online at www.liebertonline.com/tea

observed, relative to control cultures ($p = 0.016$). The matrix yield (percentage of total elastin in the matrix form, normalized to DNA) increased significantly from 1.4% (control) to 3.4% (2 μg/mL HA-o and 10 ng/mL TGF-β) $p = 0.032$).

There were no increases in tropoelastin production by aHASMCs at doses < 2 μg/mL of HA-o and 5 ng/mL of TGF-β (Fig. 5A); at higher doses, significant increases were noted relative to control cultures ($p < 0.01$ in all cases). At these higher dose combinations, a significant increase in matrix elastin production was also observed, relative to control aHASMC cultures (Fig. 5B; $p < 0.02$ in all cases). The matrix yield enhanced from 0.19% (control) to 0.31% (2 μg/mL HA-o and 5 ng/mL TGF-β; $p = 0.039$).

Ultrastructure of matrix elastin

Figure 6 shows representative transmission electron micrographs (TEM) of aRASMC layers after 21 days of culture in the absence (Fig. 6A, C) and presence (Fig. 6B, D) of elastogenic factors. Similar to that previously observed in healthy cultures of RASMCs, untreated control aRASMCs deposited sparse aggregating clumps of amorphous elastin protein and occasional immature elastic fibers (Fig. 6A, C). When TGF-β1 and HA-o together were provided to these cultures, mature elastin fiber formation was favored, with the matrix containing numerous fully formed bundles (100–200 nm in diameter) of aggregating fibrils (Fig. 6B, D). Fibrillin (immunogold particle-stained) appeared as darkly

stained nodules and was located at the periphery of aggregating elastin fiber bundles, signifying normal elastic fiber assembly (Fig. 6E).

Our study indicated that untreated (control) aHASMCs proliferate very slowly in culture. As a result, even extended periods of culture failed to generate a sufficiently dense cell layer that could be maintained intact when processed for TEM. In the absence of control cell layers for evaluating factor-treated cell layers, these results have been omitted from this article; comparison has instead been made using SEM alone.

Representative scanning electron micrographs of elastic matrices isolated from 21-day-old cultures of treated and untreated (control) aRASMCs and aHASMCs are shown (Figs. 7 and 8, respectively). As expected, the aRASMC layers contained a more dense matrix than aHASMC layers due to greater cell proliferation over the culture period and, hence, greater cell density at the time of processing for SEM. The images show that with both cell types, mature elastic fiber formation is enhanced significantly in the presence of HA-o and TGF-β factors, relative to untreated cell layers, which contained featureless clumps of amorphous elastin, and a few immature elastic fibers.

Von Kossa staining

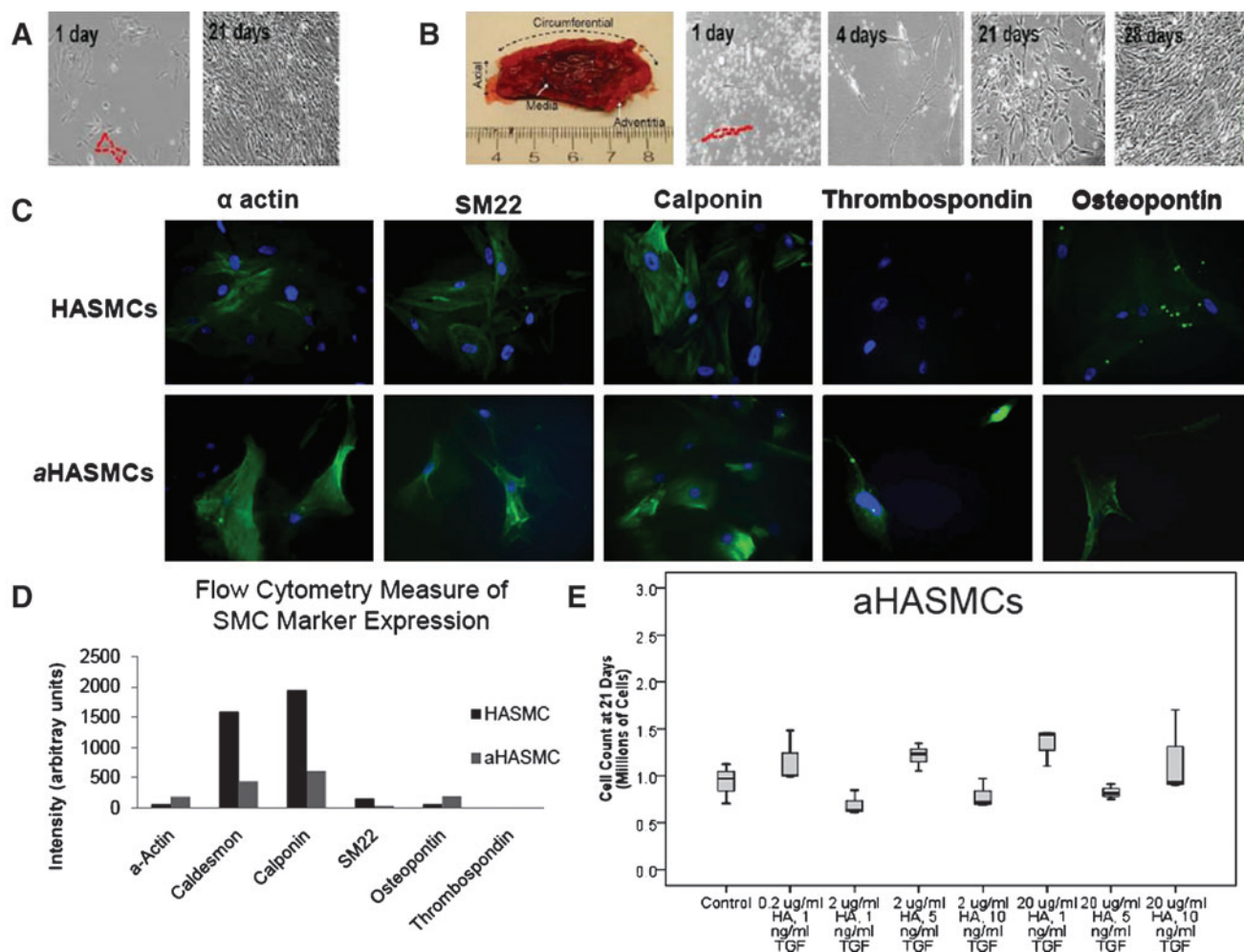Calcific deposits were minimal or absent in all of the culture groups (aRASMC, aRASMC + factors, aHASMCs,

FIG. 3. (A) Phase contrast images of primary HASMCs 1 and 21 days postseeding. (B) Phase contrast images of primary aHASMCs 1, 4 14, 21, and 28 days postseeding. (C) Immunofluorescence images comparing expression of phenotypic markers by HASMCs and aHASMCs. (D) Flow cytometry data of HASMC and aHASMC phenotypic marker expression (total intensity of marker expression per 100 cells). (E) aHASMC count after 21 days of culture with or without HA-o and TGF-β factors ($n = 3$/case). HASMCs, human abdominal aortic aneurysms-derived SMC. Color images available online at www.liebertonline.com/tea

and aHASMCs + factors) after 21 days of culture. The results indicated that there was no/minimal uptake of Ca^{2+} from the culture medium and that sustained exposure of the cell types to TGF-β at any of the doses provided did not induce matrix calcification.

Proteolytic enzyme activity

We observed a significant increase in total (i.e., of both zymogen and active forms) activity of MMPs-2 and -9 in untreated aRASMC cultures relative to healthy RASMC cultures (1.67-fold and 2.07-fold, respectively; $p = 0.03$ and 0.01),[15] confirming their activated phenotype. As shown in Figure 9, gelatin zymography analysis of spent medium aliquots from aRASMC cultures treated with the factors (2 μg/mL HA-o, 10 ng/mL TGF-β) showed MMP-2 and MMP-9 activities to be 78% ± 0% and 96% ± 1% respectively, of that in untreated aRASMC cultures.

Similar to outcomes observed with RASMCs (healthy and aneurysmal), MMP-2 activity in untreated aHASMC cultures was higher than that in healthy HASMC cultures (Fig. 10A;

1.30 ± 0.08-fold greater MMP-2 activity and 1.08 ± 0.02-fold greater MMP-9 activity). Different from aRASMC cultures, aHASMC cultures supplemented with factors (2 μg/mL HA-o, 5 ng/mL TGF-β) exhibited slightly greater MMP-2 (1.33 ± 0.11-fold increase) and MMP-9 (1.33 ± 0.11-fold increase) activities (Fig. 10B) relative to untreated aHASMC cultures. However, MMP arrays showed that elastogenic factors induced across the board decreases in amounts of several MMPs including elastolytic MMPs-2 and -9, and TIMPs-1, -2, -3, and -4 in aHASMC cultures (Fig. 10D, E).

Discussion

The long-term goal of this project is to develop methods to enhance elastic matrix regeneration within AAAs toward arresting and, possibly, even regressing their growth, thus eliminating the need for surgical intervention. This is specifically challenging, because elastin turnover is slow, and minimal remodeling of elastin fibers occurs in adults.[19] Since our elastogenic factors (HA-o and TGF-β) have been shown to be useful in stimulating elastic matrix regeneration and
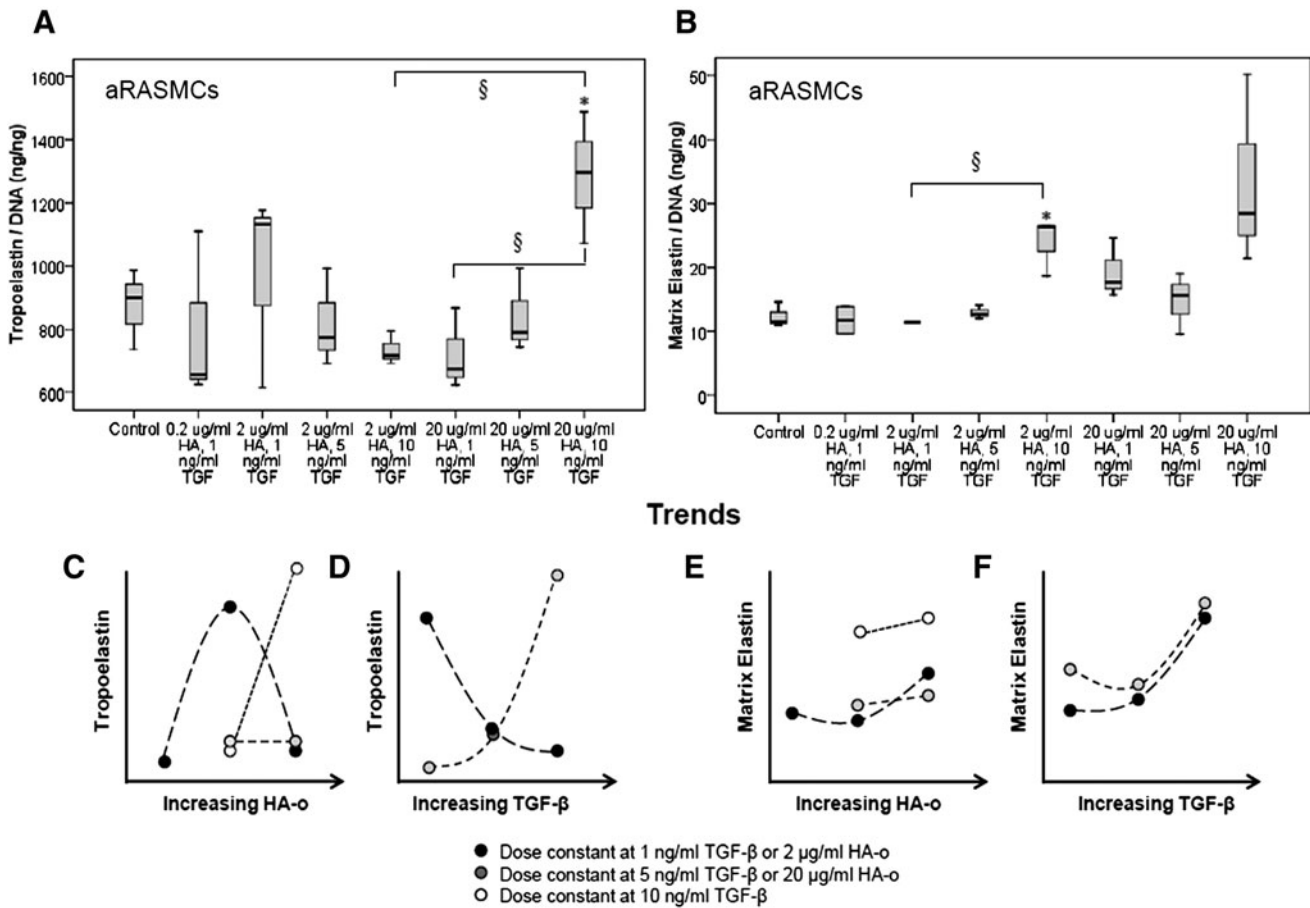
FIG. 4. Effects of HA-o and TGF-β factors on tropoelastin **(A)** and matrix elastin **(B)** production by aRASMCs. Data are shown normalized to cellular DNA content at 21 days of culture ($n=3$/case). *$p<0.05$, § indicates significance <0.01. **(C–F)** Tropoelastin and matrix elastin production trends (based on mean values) associated with increases in HA-o or TGF-β.

repair *in vitro*, we expect that they will also be useful to induce elastic matrix regeneration within intact AAA tissues to delay or regress their growth. We have investigated the feasibility of this via preliminary studies of the effects of the factors on cultured aneurysmal SMCs.

Rats are widely used to study AAAs.[20,21] Among the several models available to induce AAAs are genetically engineered animals (e.g., lysyl oxidase (LOX)-1, TIMP-1, LDL-receptor- knockout mice) and surgical/chemical induction (intraluminal elastase infusion and periadventitial injury with $CaCl_2$).[17,22] In particular, periadventitial injury of the abdominal aorta with $CaCl_2$ has been shown to induce several characteristics of human AAAs, such as medial layer disruption, inflammation, matrix calcification, thrombus formation,[22] and enhanced MMP activity at the site of application[9,16] associated with progressive, local aortic dilation within 4 weeks.[23] This model is, thus, frequently used as a surrogate accelerated study of human AAA pathology. Despite broad similarities with human AAAs, in the context of investigating elastic matrix regeneration and induction of the same by human AAA-derived SMCs, the utility of the rat model of aortal $CaCl_2$-injury remains unproved. From the standpoint of assessing the efficacy of our elastin regenerative factors for AAA treatment in animal models of disease, it is vital to ascertain that outcomes in the surrogate model/cell

type parallel outcomes in humans. Therefore, in this study, we compared the elastogenicity and elastogenic inductability of SMCs isolated from $CaCl_2$-induced rat AAAs (aRASMCs) and from atherosclerotic human AAA tissue (aHASMCs).

At 4 weeks postinjury, $CaCl_2$-treated rat abdominal aortae exhibited many characteristics typical of human AAAs, such as medial elastic matrix disruption, medial thinning, calcification, and increased MMP activity. The ∼45% increase in aortic diameter that is induced after periadventitial $CaCl_2$ injury lies within the range reported by others[17,23] and qualifies as an early AAA-like expansion.

We compared the elastogenic responses and elastogenic inductability of cultured rat and human SMCs, and not SMCs within intact tissues. The advantage of studying cells in culture is that (1) rigorous evaluation is possible without encountering tissue procurement limitations, as cultured cells can be propagated and (2) the standalone effects of individual cell-behavior-influencing factors (e.g., TGF-β and HA-o in this study) can be determined. However, evaluation of cells cultured on 2D substrates, as performed in this study, has two intrinsic limitations. The first limitation is that such cells neither experience biomechanical transductive signals such as that imposed by cyclic stretch of the vessel wall and hemodynamic pressure *in vivo* nor biochemical signals unique to healthy or aneurysmal vascular microenvironments.
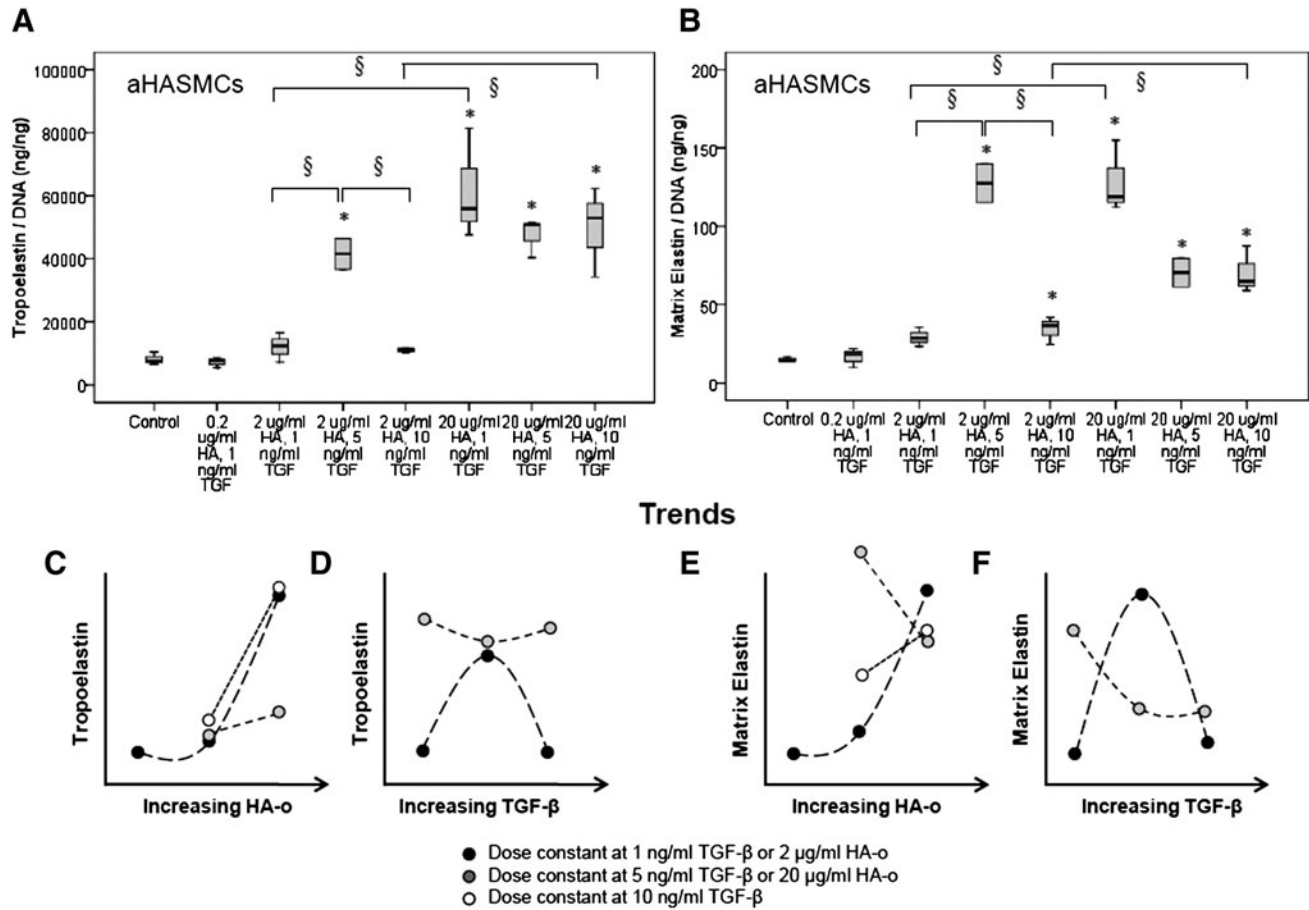
FIG. 5. Effects of HA-o and TGF-β factors on tropoelastin **(A)** and matrix elastin **(B)** produced by aHASMCs. Data are shown normalized to cellular DNA content at 21 days of culture ($n=3$/case). *$p<0.05$, § indicates significance <0.01. **(C–F)** Tropoelastin and matrix elastin production trends (based on mean values) associated with increased in HA-o or TGF-β.

The second limitation, which is well recognized in the field of tissue engineering, is that cells cultured on 2D substrates can behave differently from cells in 3D microenvironments such as the ECM-rich tissues. Previous studies have shown that in 3D fibrous microenvironments, SMCs assume a more contractile, less proliferative phenotype characterized by reduced capacity for ECM synthesis. In this first study, since we were unclear as to the elastogenic potential of human SMCs, and unsure of our ability to obtain measurable elastic matrix amounts on culture of these cells within 3D scaffolds, we deliberately investigated 2D cell cultures. We plan to use outcomes of this study to guide design of follow-up culture experiments, wherein we will investigate basal and induced elastic matrix synthesis by healthy and aneurysmal SMCs seeded either within 3D synthetic scaffolds or within *ex vivo* organ cultures of aneurysmal aorta tissues.

Differences in phenotype between healthy and aneurysmal vascular SMCs have been reported by others.[24] As determined in those studies, we also observed that aRASMCs derived from $CaCl_2$-injured aortae exhibited decreased volume/spreading and SM22, caldesmon, and calponin expression as compared with healthy RASMCs (Fig. 2A, B). SM22, a protein found extensively in adult SMCs, is implicated in restricting phenotypic changes from a contractile to a synthetic phenotype[25]; it is homologous to calponin and

can be functionally compensated by calponin in maintenance of SMC homeostasis.[26,27] Caldesmon plays a key role in SMC contraction by binding to actomyosin contractile units such as actin, tropomyosin, myosin, and calmodulin[28] and may have a regulatory role in the contractile apparatus; it has been reported to inhibit the Mg^{2+}-ATPase activity and, hence, inhibit smooth muscle contractility.[29] Calponin binds with actin filaments (F-actin) depending on the presence of Ca^{2+}, thereby regulating the contractile apparatus of SMCs[30,31]; due to this binding, it also inhibits Mg^{2+}-ATPase activity *in vitro*.[32] Together, a decrease in expression of these markers signifies a loss of contractile SMC phenotype. In addition, the aRASMCs also exhibited increased expression of osteopontin, a multi-functional pro-inflammatory cytokine implicated with vascular disease and enhanced inflammatory response[33]; osteopontin has been shown to induce chemotaxis of macrophages and monocytes, which stimulates calcification[34] and enhances MMP activity, thereby promoting vascular wall deterioration.[35] In tandem with these alterations in phenotypic marker expression, the aRASMCs exhibited enhanced activities of elastolytic MMPs-2 and −9 over healthy control RASMCs, suggesting an activated phenotype.[15]

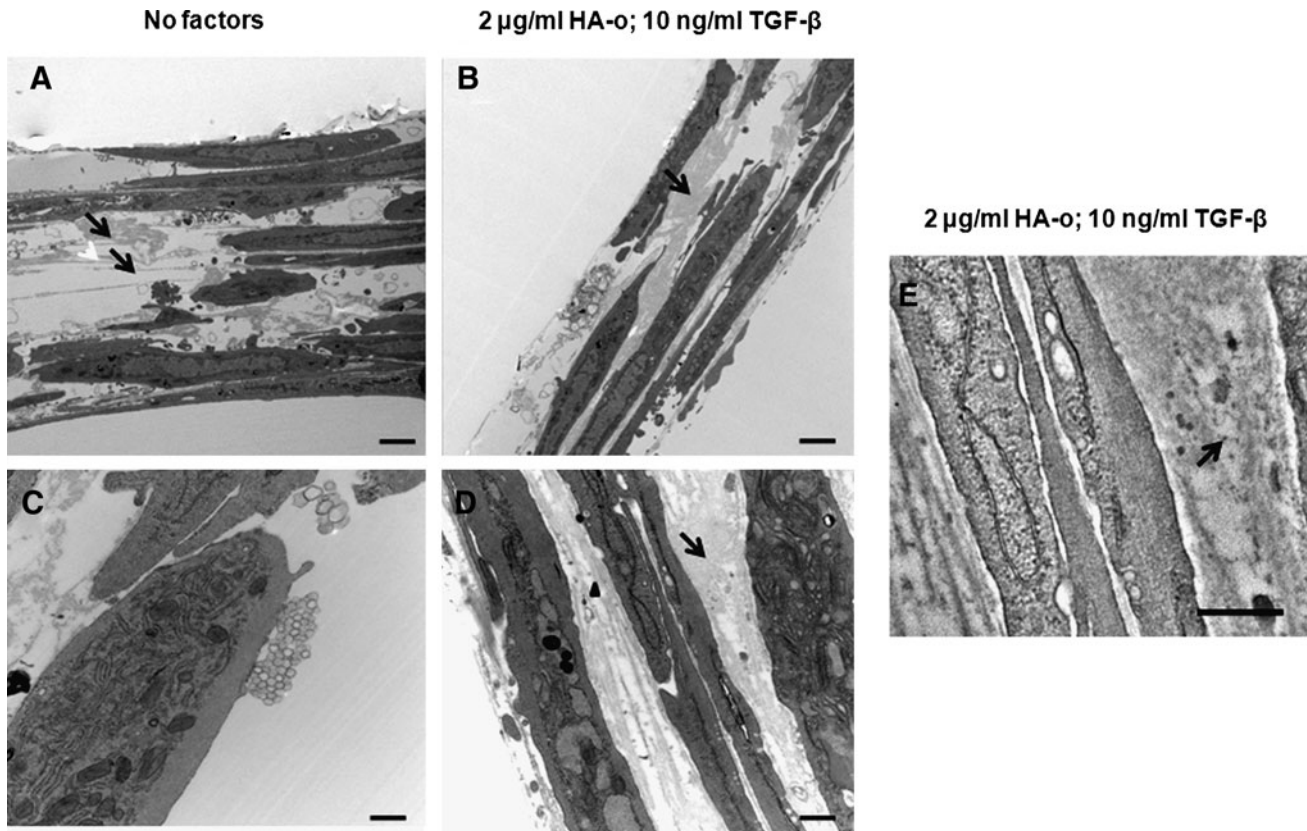Similar to aRASMCs, aHASMCs appeared to be of a less contractile phenotype than were healthy HASMCs; the

No factors

2 µg/ml HA-o; 10 ng/ml TGF-β

2 µg/ml HA-o; 10 ng/ml TGF-β

FIG. 6. Representative transmission electron microscopy images of 21-day-old aRASMC cultures with **(B, D)** or without **(A, C)** HA-o and TGF-β factor supplementation **(A** and **B:** 7,300× magnification; scale bar = 2 µm; **C** and **D:** 30,000× magnification; scale bar = 300 nm). Black arrows indicate elastic matrix. The black arrow in panel **(E)** indicates immunogold-labeled fibrillin microfibrillar proteins (scale bar = 300 nm).

aHASMCs also exhibited a marginal increase in expression of markers typical of injured/activated SMCs (e.g., osteopontin; Fig. 3C, D). The aHASMCs cells were also similar to aRASMCs in that they proliferated more rapidly than healthy HASMCs (though much slower compared with aRASMCs) and that exposure to HA-o and TGF-β at any tested dose had no impact on cell proliferation. Overall, these results show that SMCs obtained by passaging primary cells isolated from both CaCl$_2$-injury generated rat AAAs and human AAAs maintain an activated phenotype in culture, exhibit morphological and phenotypic similarities, and proliferate more rapidly compared with their healthy counterparts. A comparison of the effects of HA-o and TGF-β factors on aRASMCs and aHASMCs revealed that the factors only
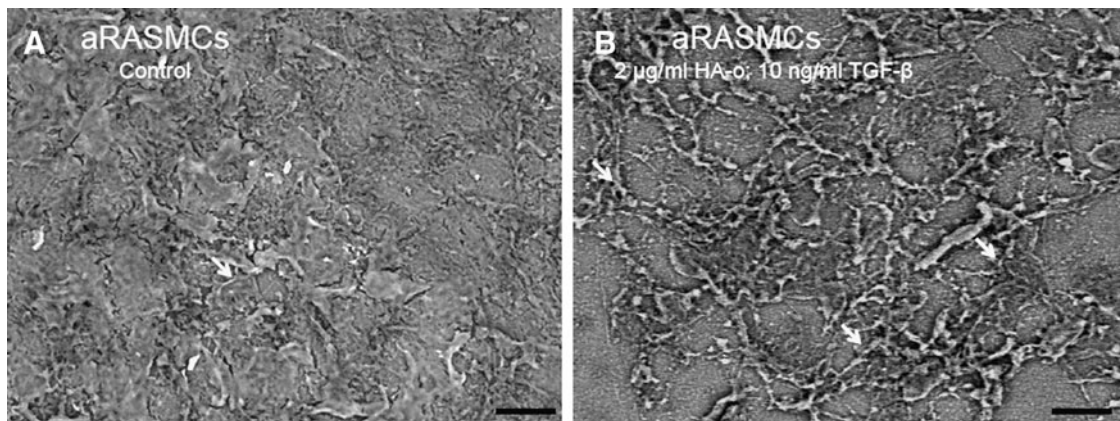

FIG. 7. Representative SEM images of elastic matrix produced by 21-day-old aRASMC cultures with **(B)** or without **(A)** HA-o and TGF-β factor supplementation (1000× magnification; scale bar = 20 µm). White arrows indicate fibrillar elastic structures. SEM, scanning electron microscopy.
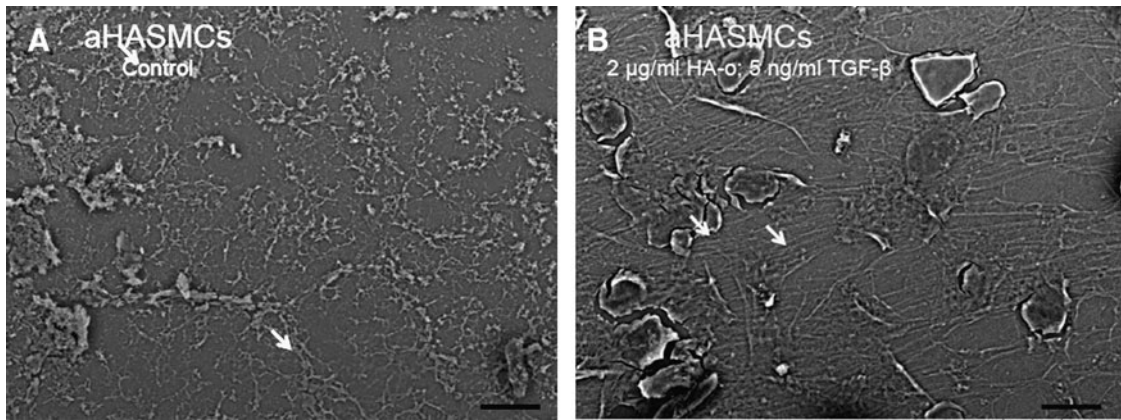
FIG. 8. Representative SEM images of elastic matrix produced by 21-day-old aHASMC cultures with **(B)** or without HA-o **(A)** and TGF-β factor supplementation (1000× magnification; scale bar = 20 μm). White arrows indicate fibrillar elastic structures.

minimally impacted proliferation of both these cell types. In aRASMC cultures, unlike in healthy RASMC cultures, low-dose combinations of HA-o ($<2\,\mu g/mL$) and TGF-β ($<5\,ng/mL$) together had no effect on tropoelastin and matrix elastin production. This agrees well with our earlier findings that diseased SMCs require higher doses of these factors for elastogenic stimulation. Also, our results indicate that HA-o and TGF-β1, in general, more sensitively influence the elastin crosslinking/matrix assembly machinery than cellular tropoelastin synthesis, which is increased only at the highest tested dose combination. At the factor doses assessed in this study, effects of TGF-β on tropoelastin production by aRASMCs were dependent on the concentration of HA-o. At low HA-o doses ($2\,\mu g/mL$), increasing doses of TGF-β (1–$10\,ng/mL$) decreased tropoelastin production, whereas at high HA-o doses ($20\,\mu g/mL$), increasing doses of TGF-β increased tropoelastin production (Fig. 4D). For a given dose of HA-o provided to aRASMCs, increasing TGF-β dose resulted in an increase in matrix elastin production (Fig. 4F). At the higher doses of TGF-β, there was a minimal effect of HA-o on matrix elastin production (see convergence of trend curves in Fig. 4F). These trends are also clearly apparent in Figure 4E, wherein dose increases in HA-o most significantly enhance elastic matrix synthesis at the lowest TGF-β dose and least at the highest tested TGF-β dose. The results with aRASMCs suggest that (1) the predominant effects of HA-o lie in the enhancement of elastic matrix deposition rather than in improvement of tropoelastin production, which corroborates inferences from our earlier studies,[13,36] (2) the effects of HA-o on matrix elastin production are most pronounced at lower tested TGF-β doses, indicating that at the highest tested TGF-β dose, TGF-β effects dominate over that due to HA-o and (c) increase in tropoelastin and matrix elastin synthesis with increasing TGF-β dose are more pronounced at higher HA-o doses.

aHASMCs showed similarities to aRASMCs in their matrix synthesis responses to the provided factors, specifically in that tropoelastin and matrix elastin synthesis were only enhanced at the higher dose combinations, and no effects were seen at the lowest doses. However, two important differences are worthy of notice. The first is that the minimal dose ($2\,\mu g/mL$ HA-o; $5\,ng/mL$ TGF-β) for significant elastogenic upregulation, particularly of tropoelastin synthesis by aHASMCs, is far lower than that determined for aRASMCs ($20\,\mu g/mL$ HA-o; $10\,ng/mL$ TGF-β). The second is that at the respective doses that induce maximal elastogenicity, the increases in amounts of tropoelastin and matrix elastin synthesized were far greater in the aHASMC cultures (5.08 ± 0.66-fold increase in ng of tropoelastin/ng DNA and 8.5 ± 1.5-fold increase in ng of matrix elastin/ng of DNA at $2\,\mu g/mL$ HA-o; $5\,ng/mL$ TGF-β) than for aRASMCs ($16\% \pm 4\%$ decrease in tropoelastin and 2.15 ± 0.28-fold
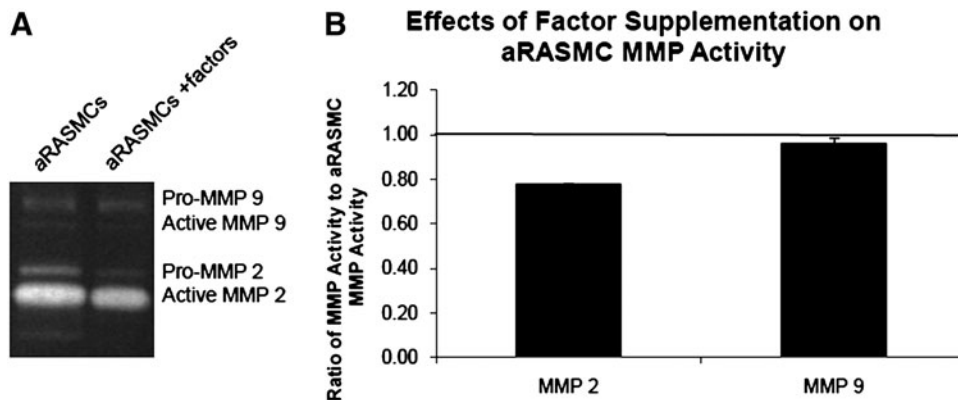

FIG. 9. **(A)** Gel zymogram showing activity of MMP-2 and MMP-9 (numerous isoforms/many bands) within aRASMC layers cultured with or without HA-o and TGF-β factors. **(B)** Data are shown normalized to the respective values observed in nonsupplemented aRASMC controls ($n = 3$/case). The factor dose assessed was $2\,\mu g/mL$ HA-o and $10\,ng/mL$ TGF-β. MMP, matrix-metalloprotease.
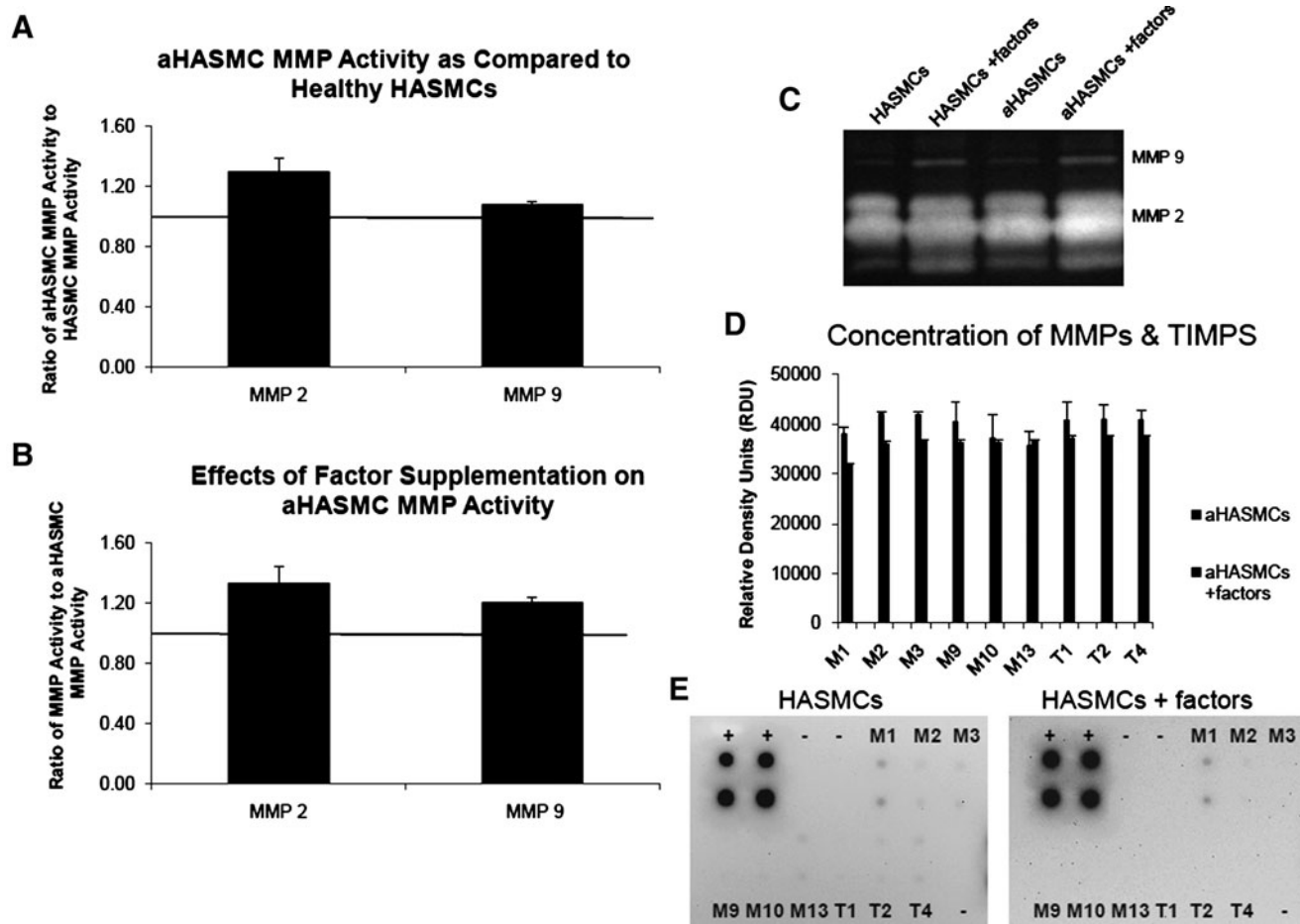
FIG. 10. Gel zymogram **(C)** showing activity of MMPs-2 and -9 (numerous isoforms/many bands) generated by aHASMCs cultured in the presence or absence of HA-o (2 μg/mL) and TGF-β factors (5 ng/mL), and by healthy HASMCs. Panel **(A)** compares MMP-2 and − 9 activities between aHASMCs and healthy HASMCs. Panel **(B)** compares the activity of MMP-2 and MMP-9 within aHASMC cultures treated with or without HA-o and TGF-β factors. Data are shown normalized to the respective controls ($n = 3$/case). **(D,E)** MMP arrays showed that the production of MMPs (MMPs-1, -2, -3, -9, -10, and -13) and TIMPs (TIMPs-1, -2, -4) released by aHASMC cultures with or without HA-o and TGF-β factor supplementation. The factor dose assessed was 2 μg/mL of HA-o and 5 ng/mL of TGF-β. TIMPs, tissue inhibitors of matrix metalloproteases.

increase in matrix elastin respectively, at 2 μg/mL HA-o and 10 ng/mL TGF-β dose combination versus untreated aRASMCs). Both these observations strongly suggest that the intracellular signaling mechanisms which form the basis for downstream outcomes of increased elastin precursor and matrix synthesis in aHASMCs are more sensitive to cell interaction with HA-o and TGF-β than in the case of aRASMCs. This is suggested from the trend curves that show elastin synthesis to have much stronger HA-o dose dependency in aHASMC cultures (at a given TGF-β dose) than in aRASMC cultures, especially at the lowest TGF-β doses (Fig. 5C, E). It is also noteworthy that at the lowest HA-o dose, TGF-β effects on elastic matrix deposition dominate, as deemed from the classic biphasic TGF-β-dose response, with an initial increase in tropo-/matrix elastin synthesis with TGF-β dose, and a sharp decrease when TGF-β dose is increased still further; such a biphasic response to TGF-β was not observed in aRASMC cultures, at least within the tested dose range (Fig. 5D, F). Our results also suggest that the provided factors encourage elastic fi-

ber organization in aHASMC cultures similar to aRASMC cultures, in a manner similar to that observed in healthy cells (Figs. 7 and 8).

At the factor dose combinations deemed most elastogenic, absolute elastic matrix amounts in aRASMC and aHASMC cultures were 149% and 57% of the elastic matrix amounts generated in untreated cultures of healthy RASMCs and HASMCs, respectively. This reveals that although elastic matrix yield is enhanced significantly, that additional elastogenic stimulation of human aneurysmal cells, in particular, may be necessary to coax cells to produce as much elastic matrix as healthy SMCs. There is, thus, a scope for further increasing matrix elastin yield. Future studies to address this challenge may incorporate combination therapies aimed at increasing crosslinking of elastin into a mature matrix. This may involve providing cells exogenous LOX to initiate covalent crosslinking of elastin precursors,[37] or alternately delivering copper nanoparticles to increase LOX activity toward improving elastic matrix yield and maturation, as we previously showed to be possible.[38,39]

Similar to aRASMCs, which exhibit enhanced MMP-2 and -9 activity relative to healthy RASMCs,[15] cultured aHASMCs also exhibited higher activity of elastolytic MMP-2 (but not MMP-9) relative to healthy HASMCs, thus confirming their activated phenotype. However, HA-o and TGF-β factors, provided at the "most effective" doses identified for the respective cell types, had very different effects on MMP activity in aRASMC and aHASMC cultures; the factors attenuated MMP-2 (minimal change in MMP-9) activity in aRASMC cultures (Fig. 9), but enhanced the same in aHASMC cultures (Fig. 10B, C), although in the latter the factors induced an across-the-board decrease in amounts of elastogenic (MMPs-2 and -9) and other MMPs relative to untreated aHASMC cultures (Fig. 10D, E).

Conclusions

In summary, our study shows that the periadventitial CaCl$_2$-injury model of AAAs exhibits many of the pathological characteristics of human AAAs. The cells isolated from such induced rat AAAAs also show similarities to human AAA SMCs including similarities in terms of decreased contractile activity, enhanced proliferation, and reduced elastogenic capacity (relative to healthy SMCs). However, the aRASMCs differ from human AAAs (aHASMCs) in their responses to elastogenic stimulation. Specifically, aRASMCs from CaCl$_2$ injury AAA models appear to be less sensitive to TGF-β and HA-o in the context of elastin regenerative responses. Although such differences in cell responses may likely be due to differences in the stage in maturation of the AAAs studied, with the CaCl$_2$-injury induced aortal expansion qualifying as a very early aneurysm and the human AAA at a more chronic stage, we also acknowledge that aHASMCs were isolated from AAA tissue from a single patient, and, thus, may not sufficiently represent phenotypic diversity of all aHASMCs. Further study of SMCs from stage-matched CaCl$_2$-injury generated aortal expansions and human AAAs will be necessary to more rigorously evaluate their basal and induced elastogenic responses. Regardless, this study suggests that a CaCl$_2$-injury model of AAAs exhibits distinctive short-comings as a surrogate in the context of elastin regeneration within human AAAs; alternate models such as an elastase-perfusion model of AAAs may be more suited for this purpose, subject to confirmation.

Acknowledgments

Disclosure Statement

No competing financial interests exist.

References

1. Selle, J.G., Robicsek, F., Daugherty, H.K., and Cook, J.W. Thoracoabdominal aortic aneurysms. A review and current status. Ann Surg **189,** 158, 1979.
2. Daugherty, A., and Cassis, L.A. Mouse models of abdominal aortic aneurysms. Arterioscler Thromb Vasc Biol **24,** 429, 2004.
3. Mecham, R.P., Broekelmann, T., Fliszar, C.J., Shapiro, S.D., Welgus, H.G., and Senior, R.M. Elastin degradation by matrix metalloproteinases. Cleavage site specificity and mechanisms of elastolysis. J Biol Chem **272,** 18071, 1997.
4. Petersen, E., Gineitis, A., Wagberg, F., and Angquist, K.A. Activity of matrix metalloproteinase-2 and -9 in abdominal aortic aneurysms. Eur J Vasc Endovasc Surg **20,** 457, 2000.
5. Lindholt, J.S., Jorgensen, B., Klitgaard, N.A., and Hennererg, E.W. Systemic levels of cotinine and elastase, but not pulmonary function, are associated with the progression of small abdominal aortic aneurysms. Eur J Vasc Endovasc Surg **26,** 418, 2003.
6. Isselbacher, E.M. Thoracic and abdominal aortic aneurysms. Circulation **111,** 816, 2005.
7. Galis, Z.S., and Khatri, J.J. Matrix metalloproteinases in vascular remodeling and atherogenesis: the good, the bad, and the ugly. Circ Res **90,** 251, 2002.
8. Keeling, W.B., Armstrong, P.A., Stone, P.A., Bandyk, D.F., and Shames, M.L. An overview of matrix metalloproteinases in the pathogenesis and treatment of abdominal aortic aneurysms. Vasc Endovasc Surg **39,** 457, 2005.
9. Isenburg, J.C., Simionescu, D., Starcher, B.C., and Vyavahare, N.R. Elastin stabilization for treatment of abdominal aortic aneurysms. Circulation **115,** 1729, 2007.
10. Isenburg, J.C., Karamchandani, N.V., Simionescu, D.T., and Vyavahare, N.R. Structural requirements for stabilization of vascular elastin by polyphenolic tannins. Biomaterials **27,** 3645, 2006.
11. Joddar, B., and Ramamurthi, A. Fragment size- and dose-specific effects of hyaluronan on matrix synthesis by vascular smooth muscle cells. Biomaterials **27,** 2994, 2006.
12. Joddar, B., and Ramamurthi, A. Elastogenic effects of exogenous hyaluronan oligosaccharides on vascular smooth muscle cells. Biomaterials **27,** 5698, 2006.
13. Kothapalli, C.R., Taylor, P.M., Smolenski, R.T., Yacoub, M.H., and Ramamurthi, A. TGF-β1 and hyaluronan oligomers synergistically enhance elastin matrix regeneration by vascular smooth muscle cells. Tissue Eng **15,** 501, 2009.
14. Kothapalli, C.R., and Ramamurthi, A. Benefits of concurrent delivery of hyaluronan and IGF-1 cues to regeneration of crosslinked elastin matrices by adult rat vascular cells. J Tissue Eng Regen Med **2,** 106, 2008.
15. Kothapalli, C.R., Gacchina, C.E., and Ramamurthi, A. Utility of hyaluronan oligomers and transforming growth factor-beta1 factors for elastic matrix regeneration by aneurysmal rat aortic smooth muscle cells. Tissue Eng Part A **15,** 3247, 2009.
16. Basalyga, D.M., Simionescu, D.T., Xiong, W., Baxter, B.T., Starcher, B.C., and Vyavahare, N.R. Elastin degradation and calcification in an abdominal aorta injury model: role of matrix metalloproteinases. Circulation **110,** 3480, 2004.
17. Chiou, A.C., Chiu, B., and Pearce, W.H. Murine aortic aneurysm produced by periarterial application of calcium chloride. J Surg Res **99,** 371, 2001.
18. Labarca, C., and Paigen, K. A simple, rapid, and sensitive DNA assay procedure. Anal Biochem **102,** 344, 1980.

19. Robert, A.M., and Robert, L., eds. Biology and Pathology of Elastic Tissues. Basel, Switzerland: S. Karger, 1980 CI, III, IV, pp. 188–195.

20. Powell, J. Models of arterial aneurysm: for the investigation of pathogenesis and pharmacotherapy-a review. Atherosclerosis **87,** 93, 1991.

21. Wills, A., Thompson, M.M., Crowther, M., Brindle, N.P., Nasim, A., Sayers, R.D., and Bell, P.R. Elastase-induced matrix degradation in arterial organ cultures: an *in vitro* model of aneurysmal disease. J Vasc Surg **24,** 667, 1996.

22. Gertz, S.D., Kurgan, A., and Eisenberg, D. Aneurysm of the rabbit common carotid artery induced by periarterial application of calcium chloride *in vivo*. J Clin Invest **81,** 649, 1988.

23. Longo, G.M., Xiong, W., Greiner, T.C., Zhao, Y., Fiotti, N., and Baxter, B.T. Matrix metalloproteinases 2 and 9 work in concert to produce aortic aneurysms. J Clin Invest **110,** 625, 2002.

24. Kondo, S., Hashimoto, N., Kikuchi, H., Hazama, F., and Kataoka, H. Apoptosis of medial smooth muscle cells in the development of saccular cerebral aneurysms in rats. Stroke **29,** 181, 1998.

25. Feil, S., Hofmann, F., and Feil, R. SM22{alpha} Modulates vascular smooth muscle cell phenotype during atherogenesis. Circ Res **94,** 863, 2004.

26. Zhang, J.C.L., Helmke, B.P., Shum, A., *et al.* SM22[beta] encodes a lineage-restricted cytoskeletal protein with a unique developmentally regulated pattern of expression. Mech Dev **115,** 161, 2002.

27. Zhang, J.C.L., Kim, S., Helmke, B.P., *et al.* Analysis of SM22{alpha}-deficient mice reveals unanticipated insights into smooth muscle cell differentiation and function. Mol Cell Biol **21,** 1336, 2001.

28. Huber, P.A.J. Caldesmon. Int J Biochem Cell Biol **29,** 1047, 1997.

29. Ngai, P.K., and Walsh, M.P. Inhibition of smooth muscle actin-activated myosin Mg2+-ATPase activity by caldesmon. J Biol Chem **259,** 13656, 1984.

30. Winder, S.J., and Walsh, M.P. Calponin: thin filament-linked regulation of smooth muscle contraction. Cell Signal **5,** 677, 1993.

31. el-Mezgueldi, M. Calponin. Int J Biochem Cell Biol **28,** 1185, 1996.

32. Winder, S.J., and Walsh, M.P. Smooth muscle calponin. Inhibition of actomyosin MgATPase and regulation by phosphorylation. J Biol Chem **265,** 10148, 1990.

33. Scatena, M., Liaw, L., and Giachelli, C.M. Osteopontin: a multifunctional molecule regulating chronic inflammation and vascular disease. Arterioscler Thromb Vasc Biol **27,** 2302, 2007.

34. Tintut, Y., Patel, J., Territo, M., Saini, T., Parhami, F., and Demer, L.L. Monocyte/macrophage regulation of vascular calcification in vitro. Circulation **105,** 650, 2002.

35. Shaheen, M., and Weintraub, N.L. Osteopontin: a bona fide mediator of abdominal aortic aneurysm? Arterioscler Thromb Vasc Biol **27,** 439, 2007.

36. Joddar, B., Ibrahim, S., and Ramamurthi, A. Impact of delivery mode of hyaluronan oligomers on elastogenic responses of adult vascular smooth muscle cells. Biomaterials **28,** 3918, 2007.

37. Kothapalli, C.R., and Ramamurthi, A. Lysyl oxidase enhances elastin synthesis and matrix formation by vascular smooth muscle cells. J Tissue Eng Regen Med **3,** 655, 2009.

38. Kothapalli, C.R., and Ramamurthi, A. Copper nanoparticle cues for biomimetic cellular assembly of crosslinked elastin fibers. Acta Biomater **5,** 541, 2009.

39. Kothapalli, C.R., and Ramamurthi, A. Biomimetic regeneration of elastin matrices using hyaluronan and copper ion cues. Tissue Eng Part A **15,** 103, 2009.

Address correspondence to:
Anand Ramamurthi, Ph.D.
Department of Biomedical Engineering
Cleveland Clinic
9500 Euclid Ave.
Cleveland, OH 44195

E-mail: ramamua@ccf.org